SANDIA REPORT

SAND2005-0189
Unlimited Release
Printed July 2005

Effects of Diesel Fuel Combustion-Modifier Additives on In-Cylinder Soot Formation in a Heavy-Duty DI Diesel Engine

Mark P. B. Musculus, Sandia National Laboratories
Jeff Dietz, The Lubrizol Corporation

Prepared by Sandia National Laboratories
Albuquerque, New Mexico 87185 and Livermore, California 94550

Sandia is a multiprogram laboratory operated by Sandia Corporation,
a Lockheed Martin Company, for the United States Department of Energy's
National Nuclear Security Administration under Contract DE-AC04-94AL85000.

Issued by Sandia National Laboratories, operated for the United States Department of Energy by Sandia Corporation.

Available to DOE and DOE contractors from
U.S. Department of Energy
Office of Scientific and Technical Information
P.O. Box 62
Oak Ridge, TN 37831

Telephone: (865)576-8401
Facsimile: (865)576-5728
E-Mail: reports@adonis.osti.gov
Online ordering: http://www.osti.gov/bridge

Available to the public from
U.S. Department of Commerce
National Technical Information Service
5285 Port Royal Rd
Springfield, VA 22161

Telephone: (800)553-6847
Facsimile: (703)605-6900
E-Mail: orders@ntis.fedworld.gov
Online order: http://www.ntis.gov/help/ordermethods.asp?loc=7-4-0#online

Effects of Diesel Fuel Combustion-Modifier Additives on In-Cylinder Soot Formation in a Heavy-Duty DI Diesel Engine

Mark P. B. Musculus
Sandia National Laboratories

Jeff Dietz
The Lubrizol Corporation

ABSTRACT

Based on a phenomenological model of diesel combustion and pollutant-formation processes, a number of fuel additives that could potentially reduce in-cylinder soot formation by altering combustion chemistry have been identified. These fuel additives, or "combustion modifiers," included ethanol and ethylene glycol dimethyl ether, polyethylene glycol dinitrate (a cetane improver), succinimide (a dispersant), as well as nitromethane and another nitro-compound mixture. To better understand the chemical and physical mechanisms by which these combustion modifiers may affect soot formation in diesel engines, in-cylinder soot and diffusion flame lift-off were measured, using an optically-accessible, heavy-duty, direct-injection diesel engine. A line-of-sight laser extinction diagnostic was employed to measure the relative soot concentration within the diesel jets ("jet-soot") as well as the rates of deposition of soot on the piston bowl-rim ("wall-soot"). An OH chemiluminescence imaging technique was utilized to measure the lift-off lengths of the diesel diffusion flames so that fresh oxygen entrainment rates could be compared among the fuels. Measurements were obtained at two operating conditions, using blends of a base commercial diesel fuel with various combinations of the fuel additives.

The ethanol additive, at 10 % by mass, reduced jet-soot by up to 15%, and reduced wall-soot by 30-40%. The other fuel additives also affected in-cylinder soot, but unlike the ethanol blends, changes in in-cylinder soot could be attributed solely to differences in the ignition delay. No statistically-significant differences in the diesel flame lift-off lengths were observed among any of the fuel additive formulations at the operating conditions examined in this study. Accordingly, the observed differences in in-cylinder soot among the fuel formulations cannot be attributed to differences in fresh oxygen entrainment upstream of the soot-formation zones after ignition.

INTRODUCTION

For more than a decade, laser diagnostics have been used to gain a better understanding of diesel combustion and pollutant formation processes. Previous work employing multiple laser/imaging diagnostics has elucidated many of the events that occur in the fuel jet of a quiescent heavy-duty diesel engine from the start of injection through the development of the premixed- and mixing-controlled-combustion phases. Observations of the fuel injection, vaporization, combustion, and pollutant formation processes of reacting diesel fuel jets were used as a basis for a conceptual model of diesel combustion, explained in detail in Ref. [1]. The following two paragraphs provide a brief overview of this conceptual model, which will be used as a basis for discussion of diesel soot formation in this paper.

Conceptual Model of Diesel Combustion - Figure 1 presents an idealized schematic of diesel combustion, adapted from Ref. [1]. This representation of diesel

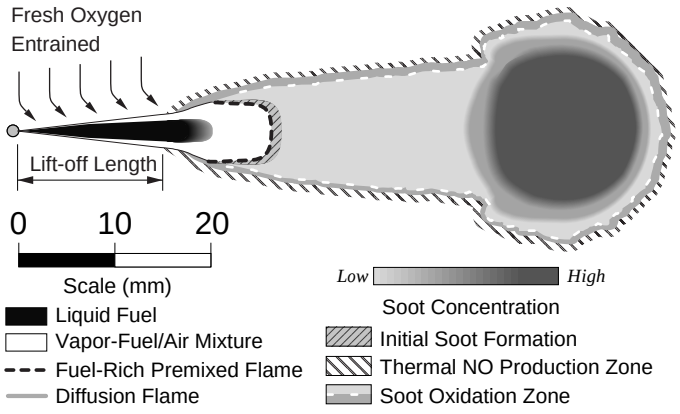

Figure 1: Schematic showing the features of a free reacting diesel fuel jet at a typical time during the quasi-steady portion of combustion, *i.e.* after the initial pre-mixed burn through the end of fuel injection. Note that unreacted oxygen is entrained only upstream of the diffusion flame lift-off length. Adapted from Ref. [1].

combustion is appropriate for typical heavy-duty diesel engines, operating at moderate- to high-load conditions. The schematic shows the main features of a "free" reacting diesel fuel jet, *i.e.,* without impingement or interaction with in-cylinder surfaces. Although the conceptual model of Ref. [1] covers the entire diesel combustion event, the schematic in Fig. 1 shows only the main "quasi-steady period" of combustion, which occurs between the end of the diesel premixed burn and the end of fuel injection. During the quasi-steady period of combustion, a turbulent diffusion flame exists around the jet periphery and extends upstream toward the injector nozzle, but typically remains detached from the nozzle. The distance between the injector nozzle and the most upstream extent of the turbulent diffusion flame is termed the "lift-off length" (see Fig. 1).

Lift-Off Length - The lift-off length has been recognized to be critically important for the formation of soot within the combusting jet, since it controls the amount of fuel-air premixing upstream of the soot formation zones in the jet [1,2]. In-cylinder gases are entrained along the whole length of the diesel jet, but downstream of the lift-off length, the fast, high temperature reactions in the diffusion flame quickly consume the ambient oxygen as it is entrained into the jet. Upstream of the lift-off length, however, no diffusion flame exists to consume the oxygen, so that fresh, unreacted oxygen is directly entrained into the jet. The hot (700-900K), fuel-rich mixture of fresh oxygen and vaporized fuel is then transported downstream of the liquid-phase fuel, where it reacts within the jet [1]. It has been hypothesized that these exothermic reactions occur in a standing premixed-combustion zone within the jet, which raises the temperature of this fuel-rich mixture as the available fresh oxygen is consumed [1].

The resulting high temperature (1300-1600 K), fuel-rich product mixture is ideal for formation and growth of soot, which occurs downstream of the (hypothesized) standing premixed reaction zone, throughout the central region of the jet [3]. Soot formation within the jet depends on the stoichiometry and temperature of the fuel-rich mixture within the jet [4]. The lift-off length can therefore affect soot formation through its influence on the amount of unreacted oxygen entrained into the diesel jet upstream of the soot-formation region. Indeed, the lift-off length has been shown to have a strong influence on soot formation in diesel jets [2,5,6]. It is conceivable that in addition to chemical effects on soot formation, fuel additives may also affect the lift-off length, which can have a physical (mixing) effect on soot formation. Therefore, measurements of the diffusion flame lift-off length are essential to quantify the effects of fuel additives on the physical mixing processes known to be important for soot formation.

The diffusion flame lift-off length can be discerned from images of naturally-occurring chemiluminescence emission. The fast, high temperature reactions occurring in the lifted, stoichiometric diesel diffusion flame have been shown to produce significant quantities of excited state OH (OH*) [7]. Accordingly, the presence of chemiluminescence emission from OH* is an indicator of the location of the diffusion flame. To measure the flame lift-off length, a technique used by Siebers and Higgins [2,7] to image OH* chemiluminescence from the reacting diesel fuel jets has been adapted and used in the facility of the current study [8]. The flame lift-off length was determined through analysis of the diffusion flame images using an intensity thresholding technique, with a mask to remove interference from liquid fuel scattering [8].

In-Cylinder Soot - The effects of fuel additives on diesel soot may be quantified by measurements of either in-cylinder or exhaust soot. These two approaches measure different aspects of the diesel soot evolution. In the exhaust stream, the amount of soot depends on the net difference between soot formation and soot oxidation processes. Measurements of in-cylinder soot, by contrast, can be tailored to directly measure soot within the diesel jets during the soot formation processes, both before and after significant oxidation occurs. Since it is the objective of the current study to isolate the effects of fuel additives on soot formation processes alone, in-cylinder soot measurements are most appropriate.

Optical extinction diagnostics that rely on the attenuation of incident radiation by soot particles may be used to quantify "jet-soot", *i.e.,* in-cylinder soot within the combusting diesel jets. A number of investigations have employed laser-extinction techniques to measure soot in diesel engines (*e.g.,* see Refs. [9-12]). Recently, the effects of fuel-bound oxygen and aromatic content on soot formation were examined using a laser extinction diagnostic in the facility of the current study [13]. The jet-soot was observed to decrease proportionally with increasing oxygen content of paraffinic fuel blends. With real diesel fuels, accurate jet-soot measurements were not possible because the soot cloud became too optically dense, and extinction laser beam was attenuated below measurable levels. Although laser-extinction diagnostics cannot directly measure optically dense jet-soot, they can be used to measure deposition of soot on in-cylinder surfaces, even for the most highly sooting fuels and conditions.

Deposition of soot on in-cylinder surfaces occurs when the sooty portion of the diesel jet impinges on the piston bowl and/or cylinder-walls. Previous studies have shown that as the jet encounters the piston bowl wall, the diffusion flame flattens along the wall surface, and is extinguished after a short time [14]. This allows the jet-soot to impinge directly onto the wall and be deposited, forming "wall-soot." In a study of in-cylinder soot formation for a range of oxygenated fuels, the rate of wall-soot deposition was observed to increase proportionally with the amount of jet-soot [11]. These results suggest that measurements of wall-soot can be used as an indicator for jet-soot under conditions for which the jet-soot is too optically dense to be measured directly. Incidentally, in that study, only minor differences in the lift-off length were observed among the fuel

blends. Accordingly, the changes in in-cylinder soot formation for those fuels were attributed primarily to chemical effects of the oxygen and aromatic content of the fuels on soot formation.

Over the past few decades, many alternative fuels and fuel additives formulations have been pursued to help reduce diesel pollutant emissions. A variety of oxygenated fuels, which contain oxygen atoms bound to carbon atoms within the fuel molecule, have been shown to influence exhaust soot emissions. References [15] and [16] contain recent reviews of many oxygenated fuel studies. Overall, most studies show that increasing oxygen content in the fuel yields decreases exhaust-soot emissions under many operating conditions. Furthermore, many studies show that the structure of the fuel molecule affects diesel soot, and fuels with similar oxygen content but different molecular structure can have significantly different effects on diesel soot [6,15,17]. Other configurations of oxygen within the fuel molecule for which oxygen is not bound to any carbon atoms may also affect soot formation. For example, nitro-compounds like nitromethane, which has a significant influence on fuel ignition chemistry [18], could also have a significant effect on in-cylinder soot formation chemistry.

In the current study, the chemical and physical parameters affecting soot formation were studied in an optically accessible, heavy-duty diesel engine. Eight different fuels with various additive formulations were used at two different operating conditions. Measurements of both jet-soot and wall-soot were used to compare the soot formation among the fuels studied. Additionally, an OH chemiluminescence imaging diagnostic was used to measure the diesel flame lift-off length to assess the influence of unreacted oxygen entrainment on soot formation.

A complete description of the engine, operating conditions, and diagnostics is given in the next section. Then, the results are presented in three parts. First, the results of laser-extinction measurements of soot within the jet are presented. Second, measurements of wall-soot deposition are presented to complement the measurements of jet-soot. Third, the diesel flame lift-off lengths, measured using OH chemiluminescence imaging, are compared among the fuels. The results are followed by a discussion, and in the final section, the results are summarized and conclusions are drawn.

EXPERIMENTAL SETUP AND DIAGNOSTICS

ENGINE – A single-cylinder, direct-injection, 4-stroke diesel engine based on a Cummins N-series production engine was used in this investigation (see Fig. 2). The N-series engine is typical of heavy-duty diesel engines, with a bore of 140 mm and a stroke of 152 mm. These dimensions are retained in the optically accessible engine, and the intake port geometry of the production cylinder head is preserved. The in-cylinder flow field of a similar Cummins N-series research engine has been examined under motored conditions and found to be nearly quiescent, with a swirl number of about 0.5 [19]. To provide optical access, the engine is equipped with an extended piston and piston-crown window, and one of the two exhaust valves is replaced with a window in the cylinder head. Windows located around the top of the cylinder-wall provide cross-optical access for the horizontal laser extinction measurements used in this study. To allow laser-extinction measurements of soot-wall deposition, an additional window was installed in the piston bowl-rim, in-line with one of the cylinder-wall windows. The opposite side of the bowl rim was cut out to allow the laser beam to pass through the cylinder without additional optical obstruction. Figure 3 presents a schematic of the combustion chamber of this engine, showing the orientation of the windows, horizontal laser beams, and the camera field of view. Finally, this optical engine is designed so that the upper cylinder liner separates and drops down from the head without engine disassembly, allowing rapid cleaning of in-cylinder surfaces. The specifications of this engine are summarized in Table 1, and additional details regarding the engine and its specifications may be found in Refs. [1,20].

Table 1. Optical Engine Specifications

Engine base type	Cummins N-14, DI diesel
Number of cylinders	1
Cycle	4-stroke
Number of intake valves	2
Number of exhaust valves	1*
Combustion chamber	Quiescent, direct injection
Bore	139.7 mm [5.5 in]
Stroke	152.4 mm [6.0 in]
Bowl width	97.8 mm [3.85 in]
Displacement	2.34 liters [142 in^3]
Connecting rod length	304.8 mm [12.0 in]
Piston pin offset	None
Geometric compression ratio	10.7:1
Simulated compression ratio	16:1

* In this optically accessible diesel engine, one of the two exhaust valves of the production cylinder head was replaced by a window and periscope

This research engine is equipped with a Cummins CELECT™ electronically-controlled fuel injector. This closed-nozzle unit injector uses camshaft actuation to build injection pressures and a solenoid-actuated valve to control injection timing and duration. For the experiments presented here, the production 8-hole injector nozzle tip was replaced with a 7-hole tip, for which one hole was “missing.” The diameters of the two holes on either side of the missing hole were increased from the original 0.194 mm to 0.238 mm so that the total flow rate and injection pressure characteristics of the production injector nozzle were maintained. This custom tip was oriented so that the fuel jet of interest (emanating from one of the 0.194 mm holes) was aligned with the bowl-rim window, while the “missing” jet was aligned with

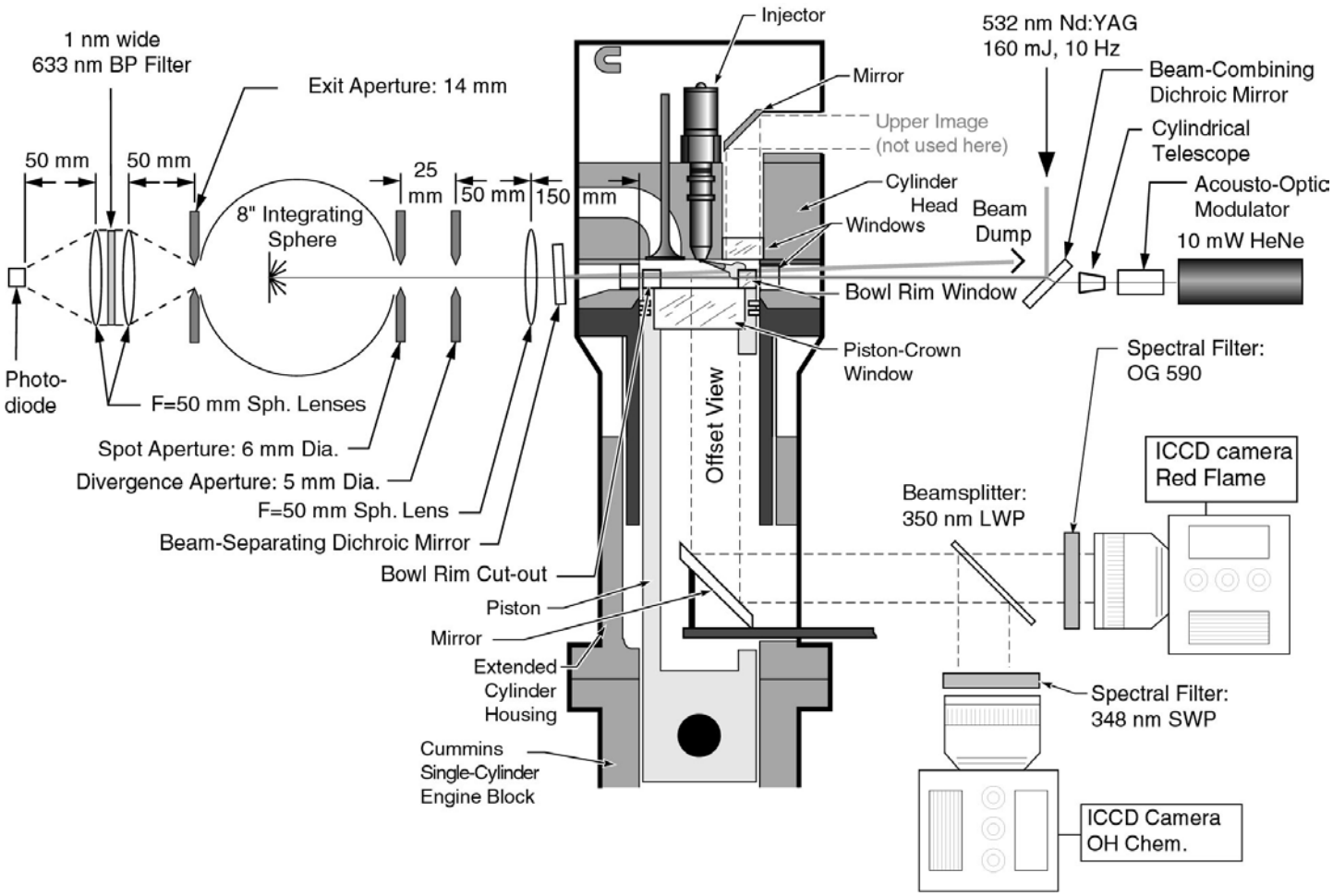

Figure 2: Schematic diagram showing optical engine, elements of horizontal LOS extinction technique, and OH chemiluminescence imaging cameras.

the cut-out in the bowl rim, as shown in Fig. 3. The fuel jet axes for this nozzle are declined 14° from the firedeck (152° included angle). The injector is instrumented with a Hall-effect needle lift sensor, and injection pressure is determined from strain gage measurements of the force on the pushtube that activates the injector. The injection pressure and cam profile are typical of those of N-series production engines. Table 2 summarizes the specifications of the fuel injector.

FUELS – A total of eight fuels were used in this study. Properties of the base diesel fuel (D2), to which all of the additives were mixed, are shown in Table 3. The seven additive fuels blends are shown in Table 4. The first four fuel additive formulations were typical of many oxygenated fuels, having oxygen bound directly to

Table 2. Specifications of CELECT™ Fuel Injector

Type	Cummins CELECT™
Design	Closed-nozzle, unit injector
Number of holes x diameter [mm]	5 x 0.194, 2 x 0.238
Length/diameter of 0.194 mm holes (l/d)	4.1
Angle of fuel-jet axes from firedeck	14°
Short-injection-duration [CAD]:	5
Mean injection pressure [MPa]:	50
Long-injection-duration [CAD]	21
Mean injection pressure [MPa]:	65

Table 3. Base Fuel Properties

Specific Gravity	.8484
Cetane Number	56.8
Viscosity	3.26 cSt
Higher Heating Value	45.73 MJ/kg
Sulfur	399 ppm
Mono Aromatics	15 %
Poly Aromatics	10.9 %
Distillation	
Initial Boiling Point	222 C
5% Point	238 C
10% Point	245 C
20% Point	254 C
50% Point	278 C
80% Point	310 C
90% Point	328 C
95% Point	344 C
End Point	346 C

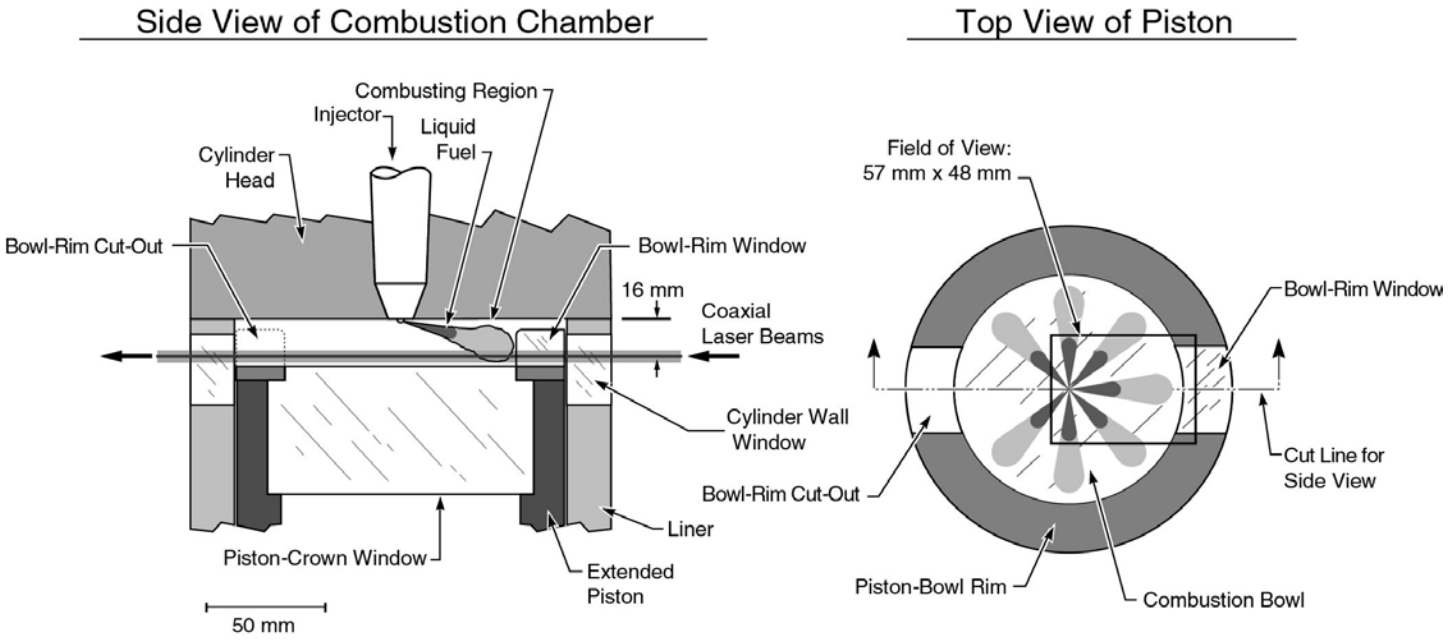

Figure 3: Schematic of the combustion chamber showing the orientations of the laser beams, the camera field of view, and the injector nozzle hole pattern

carbon atoms in the additives. These fuel blends were expected to affect soot formation in a similar way to that observed for other oxygenated fuels [6,13,15,17]. Ethanol was added to the first three of the these conventional oxygenated fuels, using a small amount of succinimide (a dispersant). The first ethanol fuel, E10, contained 10% ethanol by weight. The addition of ethanol to diesel fuel yielded a reduction in the cetane number and an increase in the ignition delay. To offset this effect, a 2.5% by weight of a cetane-improving additive, polyethylene glycol dinitrate (PEGDN), was added to the second ethanol fuel, EP10, displacing some of the ethanol (see Table 4). The third ethanol fuel, EG10 contained 10% ethanol and 0.5 % ethylene glycol dimethyl ether (EGDE). The fourth additive fuel, G05, contained 0.5 % of EGDE only. The fifth and sixth fuels, NE05 and NM05, contained small quantities of nitro compounds, as indicated in Table 4. The NE05 fuel contained 0.5% of a compound labeled as 2002-20605, the composition of which is included at the bottom of Table 4. The NM05 fuel contained 0.5% nitromethane. These fuel additives were selected because the oxygen is not bound to carbon atoms within the fuel molecules, and might therefore be more available to oxidize soot precursors and inhibit soot formation within the diesel jet. The final fuel, S05, contained 0.5% succinimide. The dispersant additive (without ethanol) was examined to study its effect on soot-wall deposition, since it was believed that it could affect soot deposition on in-cylinder surfaces.

Table 4. Fuel Additive Formulations

Fuel	Composition (by weight)	Oxygen (Wt. %)	GIMEP (kPa) Low-Load	GIMEP (kPa) High-Load
D2	Base Diesel Fuel	~0	140	1020
E10	10 % Ethanol	3.5	125	970
EP10	7.5 % Ethanol, 2.5 % PEGDN	~3.5	130	985
EG10	10 % Ethanol, 0.5 % EGDE	3.5	120	970
G05	0.5 % EGDE	0.18	135	1010
NE05	0.5 % 2002-20605* nitro-compound	<0.5	135	1020
NM05	0.5% nitro-methane	0.26	140	1015
S05	0.5% succinim-ide dispersant	0.16	140	1025

*2002-20605 contains, by weight, 7.1% alkyl aminoester, 40% polyolefin aminoester, 9.26% ammonium nitrate, 23.8% 2-Ethylhexyl nitrate, and 19.8% polyolefin amide alkeneamine.

OPERATING CONDITIONS – All data were acquired at an engine speed of 1200 rpm, at two representative diesel engine operating conditions, characterized by their gross indicated mean effective pressures (GIMEP). As shown in Table 5, the estimated motored top dead center (TDC) temperature and density were 817 K and 18.8 kg/m^3 for the low-load (135 kPa GIMEP) operating condition, and 835 K and 23 kg/m^3 for the high-load (1000 kPa GIMEP) operating condition. These TDC conditions were estimated assuming a polytropic compression from the intake manifold conditions with a

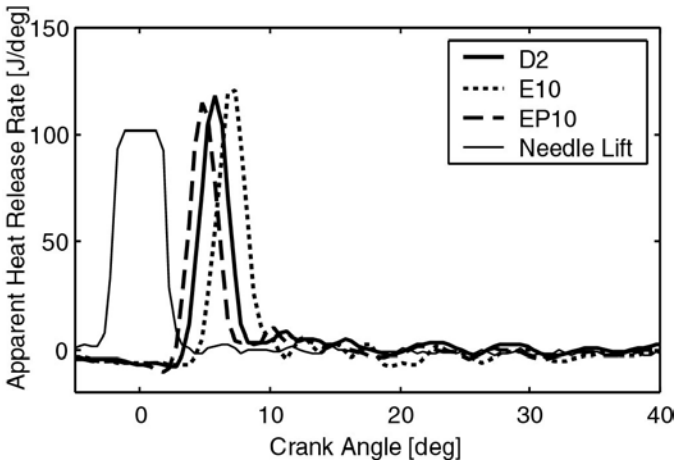

(a)

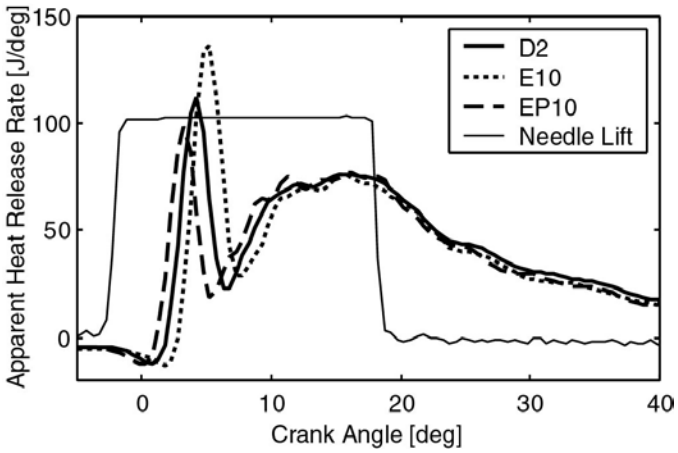

(b)

Figure 4. AHRR and fuel injector needle lift signal [a.u.] for D2, E10, and EP10 at (a) the low-load, and (b) the high-load conditions.

coefficient of 1.36. These two operating conditions are roughly equivalent to modes 1 and 3 of the AVL 8-mode steady state engine test matrix. Because modifications for optical access resulted in a compression ratio of only 10.7:1[1], as compared to approximately 16:1 for a production engine, the intake air pressure and temperature were elevated above typical levels to achieve these TDC conditions. Although these TDC conditions are representative of production hardware, the optical engine has a slightly hotter, denser air charge away from TDC because of the lower geometric compression ratio. The mass of the air charge is also somewhat greater than that of the production engine due to the larger clearance volume.

In our previous soot-wall interaction studies, the temporal history of the soot-wall interaction was shown to have a significant impact on the rate of soot-wall deposition [12,14]. Accordingly, the injection duration, rather than the engine load, was chosen as the parameter maintained constant for each of the tests in this study. The temporal development of the combusting fuel jet and the history of the soot-wall interaction between fuels were thus matched as closely as possible, though the engine load (GIMEP) varied slightly due to differences in fuel chemical energy content and combustion phasing.

Before conducting the experiments, the engine was heated to 368 K (95° C) by means of electrical heaters on the "cooling" water and lubricating oil circulation systems. To avoid overheating, the optical engine was fired once every 10th engine cycle. A 75 hp electrical motor maintained a constant engine speed between fired cycles.

Figure 4 shows the needle lift signals and the apparent heat release rates (AHRR) for three of the fuels at both operating conditions. For clarity, the AHRR data for EP10, D2, and E10 only are included in Fig. 4. These three fuels are representative of the behavior observed with the range of fuels in the current study, since they display the shortest, an intermediate, and the longest ignition delays, respectively. Since the injection duration, rather than engine load, is maintained constant among fuels, differences in the chemical energy contents and ignition delays of the fuels result in small differences in the individual AHRR curves for each of the fuels. For instance, the fuels with longer ignition delays, such as E10, display a larger premixed burn spike, especially at high-load (see Fig. 4). The resulting engine output power (GIMEP) varies slightly among the fuels because of differences in combustion phasing and fuel chemical energy content (see Table 3).

DIAGNOSTICS

Horizontal LOS Extinction – The laser extinction diagnostic was based on a line-of-sight (LOS) technique developed previously in this laboratory [10-13]. As shown in Fig. 2, the red (633 nm) output beam of a 10 mW continuous wave (CW), linearly polarized HeNe laser was directed horizontally though the combustion chamber, 16 mm below the firedeck. At this elevation, the LOS beam is well below the liquid fuel-sprays emanating from the injector, so they do not interfere with the transmission of the beam. The beam passed though

Table 5. Engine Operating Conditions

	Low-Load	High-Load
Engine Speed [rpm]	1200	1200
Nominal GIMEP [kPa]	135	1000
TDC Temperature* [K]	817	835
TDC Density* [kg/m3]	18.8	23

* The TDC conditions were estimated assuming a polytropic compression from the intake manifold conditions with a coefficient of 1.36.

[1] The engine geometry is identical to that used in previous studies [1,11,12,14,20], for which the reported compression ratio was 10.5:1 . Subsequent analysis indicated that the actual compression ratio is 10.7:1.

two cylinder-wall windows, and, when the piston was near TDC, through the bowl-rim window and the cut-out opposite of the window, as discussed above (see Fig. 3).

When measuring either jet-soot or wall-soot on the piston bowl-rim window, soot deposits on the cylinder-wall windows may interfere with the desired measurements. To remove soot deposits from the cylinder-wall window surfaces, a high power pulsed YAG laser beam was directed through the chamber coaxially with the path of the HeNe beam. As shown in Fig. 2, a 45°-incidence dichroic mirror was used to combine the two beams. To separate the beams after they passed through the engine, a normal-incidence dichroic mirror was installed such that the YAG beam reflected back through the combustion chamber slightly off-axis and into a beam dump, as shown in Fig. 2. The HeNe beam passed through both dichroic mirrors and into the integrating sphere. The YAG laser was operated at 10 Hz, and the 160-mJ second harmonic pulses (532 nm), with an unfocused a diameter of about 12 mm, were found to be sufficient to remove the soot deposits from the cylinder windows. For soot-wall deposition measurements, the pulses were timed such that the cylinder-wall windows were cleaned of soot at –60 CAD ATDC each engine cycle, when the bowl-rim window was not in the path of the beam. For the jet-soot measurements, the YAG laser was fired near TDC to clean soot deposits from the bowl-rim window also, and the timing was varied such that the entire surface of the bowl-rim window was cleaned over the 10 engine cycles between each fired cycle. Thus, the bowl rim-window was completely cleaned of soot-wall deposits before each fired cycle. This allowed jet-soot attenuation measurements to be acquired without significant attenuation from wall-soot deposits on the bowl-rim window.

The other optical elements in Fig. 2, including the cylindrical telescope, collection lens, divergence and spot apertures, integrating sphere, and narrow bandpass filter assembly were employed to minimize laser etaloning effects, account for beam steering, and reject background combustion luminosity. A complete discussion of the mechanisms by which these optical elements correct for these interferences is lengthy, and is beyond the scope of this paper. A detailed description, however, is included within Refs. [13,21].

The transmissivity of the soot cloud was defined as the ratio of the transmitted intensity during a fired cycle to that for a motored cycle:

$$\tau = \frac{\left(I_{LaserOn} - I_{LaserOff}\right)_{Fired}}{\left(I_{LaserOn} - I_{LaserOff}\right)_{Motored}} \qquad (1)$$

Here, τ is the transmissivity, and I is the transmitted LOS beam intensity. Combustion luminosity from hot soot can be quite significant under some operating conditions, reaching up to 5 % of the full-strength laser intensity. To correct for combustion luminosity that leaks through the collection system, the measured intensity with the laser off was subtracted from the intensity with the laser on, as shown in Eq. 1. An acousto-optic modulator (AOM) was used to shutter the LOS laser quickly, once for each shaft encoder tick (1/2 CAD resolution). Additionally, data were acquired during one motored cycle immediately before each fired cycle, to provide the baseline signal levels for the denominator of Eq. 1.

The LOS transmittance data was converted to a relative measure of the amount of jet-soot using a form of Beer's Law [22]:

$$KL = -ln(\tau) \qquad (2)$$

The product KL is a measure of the optical density (on a natural log scale) of jet-soot along the path of the LOS beam. The applicability of Beer's law for measuring both jet-soot and soot-wall deposition was discussed in detail in one of our previous LOS attenuation studies [12][2].

Note that when optical attenuation of the LOS beam was great, minor noise in the intensity data resulted in some near-zero or even small negative values for the relative transmittance, yielding undefined values for KL. To allow KL values to be calculated for this data, an artificial lower limit corresponding to $KL = 10$ was applied to each relative transmittance data point. As will be shown later, this KL limit truncates the data to values less than KL=10, especially for highly sooting fuels at the long-injection duration operating condition. Discussion of the uncertainty in the KL data for such optically thick soot clouds is deferred to the Results section.

Similarly, Beer's Law can be applied to obtain a relative measurement of the amount of soot deposited on the bowl-rim window. As discussed above, during the wall-soot measurements, the YAG laser cleaning-pulses were timed such that they cleaned the cylinder wall windows, but did not clean the piston bowl rim window, onto which the soot was deposited. The thickness of the soot deposit on the window surface increased with each fired cycle. Accordingly, the KL of the window deposit was evaluated while the piston was near TDC during the motored cycle following each fired cycle [13]. In previous measurements of the wall-soot deposition, the rate of accumulation was found to be nearly linear for the first 10-100 fired cycles [13]. Similar behavior was observed in the current study, and the rate of deposition (change in KL per cycle) was determined using a linear curve-fit over those cycles within the linear deposition range.

OH Chemiluminescence Imaging – As discussed in the introduction, the fast, high temperature reactions occurring at the lifted, stoichiometric diffusion flame produce significant quantities of excited-state OH. The chemiluminescence emission from these excited OH

[2] In a previous study [11], planar laser-Induced incandescence data were used to estimate the path length, L, and thus determine K to estimate soot concentrations.

radicals was used in this study as an indicator of the location of the diffusion flame. Measurements of the lift-off length are only meaningful during the quasi-steady period of diesel combustion, which occurs between the end of the premixed burn and the end of injection. As shown in Fig. 4, the injection event ends before the peak in the premixed burn for all of the low-load conditions, so the lift-off length is not meaningful and it was not measured for the low-load conditions. Hence, the lift-off length was measured for only the high-load conditions, which display a significant quasi-steady combustion period. A two-camera simultaneous imaging technique was used to measure the lift-off length, as explained in detail within Ref. [8]. A brief description of the OH chemiluminescence imaging diagnostic for measuring lift-off length is provided in the following paragraphs.

The OH chemiluminescence signal during each fired cycle was collected through the piston-crown window by a UV-sensitive, gated, intensified, charge-coupled-device (ICCD) camera, equipped with a Nikon f/4.5 UV lens. The ICCD camera had a video chip resolution of 760 by 480 pixels, and a PC-controlled frame grabber with a resolution of 640 by 480 pixels digitized the analog video output. A personal computer and digital delay generators controlled synchronization between the engine, lasers, cameras, and intensifier gates, with the master signal coming from the engine shaft encoder. Due to speed limitations of the laser and video recording system, only one image could be acquired per cycle. Previous imaging experiments have shown that the lifted diffusion flame forms shortly after the peak in the premixed burn spike in the AHRR. Characteristic OH chemiluminescence images were therefore acquired about 2 CAD after the peak in the premixed burn spike. A 348-nm short-wave-pass filter was placed in front of the camera lens to isolate the OH chemiluminescence from other emission.

Although OH chemiluminescence is the dominant source of UV emission near 310 nm [7,23], other sources of interference can be significant, especially visible light that is scattered off the liquid fuel spray [8,13]. To remove this scattering interference, a second camera was used to acquire a simultaneous image of long-wavelength light emitted by the flame. A 350 nm long-wave-pass (LWP) beam splitter and an OG590 color glass filter were employed to separate the beams and isolate the red flame emission, as shown in Fig. 2. Broadband incandescence from hot soot is the primary source of the red flame emission, which typically occurs downstream of the flame lift-off length. Liquid-scattering interference is present in both the OH chemiluminescence images and the red flame emission images. Since the OH chemiluminescence and red flame emission are spatially separated near the lift-off length, the red flame image may be subtracted from the OH chemiluminescence image to remove the liquid scatter interference without disrupting the flame structure near the lift-off length. After removal of the liquid scatter interference, an intensity thresholding scheme was used to extract the lift-off length from the images, as described in Ref. [8].

Cylinder Pressure and Heat Release Rate – In addition to the optical diagnostics, cylinder pressure, injector needle lift, and injector push-tube force (from which the fuel-injection pressure is derived) were digitized at half-CAD increments for each fuel/operating condition. Using a typical first law and perfect gas analysis (see for example Heywood [24]), the AHRR were calculated from the pressure data for each cycle and ensemble averaged. Prior to calculating the AHRR, pressure data were smoothed with a Fourier series high-frequency-reject filtering algorithm that used a Gaussian roll-off function as discussed in Ref. [25].

RESULTS

JET-SOOT EXTINCTION – The transmissivity of the jet-soot was measured using the horizontal LOS extinction technique described above for each of the fuels at both the low-load and high-load operating conditions. Shown in Fig. 5 are jet-soot transmissivity and KL for the base diesel fuel (D2) at both operating conditions, the ensemble-averaged over 192 fired cycles. For reference, the AHRR for each of these conditions, is also included on each plot (dotted line). For the low-load condition, evidence of attenuation of the LOS laser is first observed about half way through the premixed burn spike of the AHHR curve, when the jet-soot transmissivity first drops below 1.0. Over the next 5-10 CAD, the transmissivity drops to about 0.8, and then increases back to about 1.0 over the next 10 CAD as the quantity of jet-soot within the path of the LOS beam decreases. The recovery of the transmissivity to nearly 1.0 is likely due to oxidation of the soot, expansion of the cylinder contents, and possible transport of the jet-soot out of the path of the LOS beam. For the relatively low-sooting low-load condition, the jet-soot KL reaches a peak value of about 0.4 (solid curve with error bars in Fig. 5). Note that a sharp increase in the apparent KL occurs near 27 ATDC, but this is an artifact caused by temporary deflection of the LOS beam as the top of the bowl rim window on the piston passes through the path of the beam.

The transmissivity and KL for the high-load condition with the base fuel display much greater attenuation than the low-load condition, as shown in Fig. 5 (b). The transmissivity drops to nearly zero, and the KL values become very large. Because the KL varies as the log of the transmissivity, uncertainty in KL becomes significant as the KL values become large. The uncertainty in the KL data is ultimately limited by the finite digitization resolution of the recording equipment, as discussed in Ref. [13]. For the equipment used in the current study, the digitization uncertainty increases from about 3% at KL = 4 to 20% at KL = 6, and is even larger for KL values greater than 6. This digitization uncertainty represents the best-case scenario; it is the lowest achievable uncertainty for the cleanest of data. Although transmissivity data can be readily acquired even for optically thick jet-soot, very small errors or noise in the transmissivity data at low signal levels can yield large errors in the calculated KL data. Accordingly, noise

levels were maintained below ± 1-2 counts by careful shielding of transmission lines and amplification of the low-current photodiode signal as close to the detector as possible. Even so, for an individual engine cycle, data above KL= 6 in Fig. 5 (within the shaded region) must be considered highly uncertain.

Although uncertainty in the KL data for individual cycles can be significant for the high-load condition, statistical analysis of multiple engine cycles can yield greater certainty in the mean behavior of the data. Using standard statistical techniques, which assume a symmetric Gaussian distribution about the mean value [26], the uncertainty in the mean KL for the ensemble of 192 cycles was calculated. The error bars in Fig. 5 represent the width of the 95% confidence interval in the mean of the KL data, based on cycle-to-cycle variation only. Cycle-to-cycle variation in the jet-soot KL was significant, and was likely caused by both real variation in the jet-soot and noise in the transmissivity data, which causes greater variation for high KL (low transmissivity) conditions.

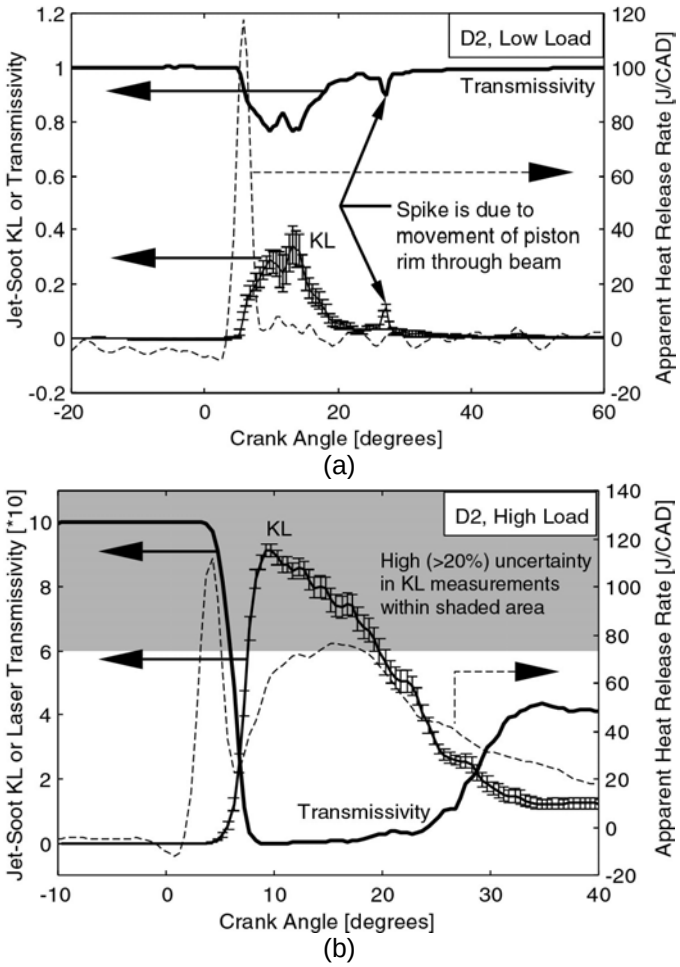

Figure 5. Transmissivity (solid line), jet-soot KL (solid line with error bars) and AHRR (dotted line, for reference) for the base diesel fuel (D2) at a) the low-load operating condition, and b) the high-load operating condition. The error bars represent the 95% confidence interval in the mean of 192 cycles, based on cycle-to-cycle variability only.

The other seven fuels studied showed similar behavior at both low- and high-load. Transmissivity and KL data similar to that shown in Fig. 5 for all of the other seven fuels are included in the appendix.

Integrated Jet Soot - As a means to compare the jet-soot levels among the various fuels examined, the time-integral of the cycle-averaged jet-soot KL was calculated. As employed here, the integrated jet-soot KL is the area under the KL versus CAD curve, such as that shown for D2 in Fig. 5. The limits for this integration were the bounds of the portion of the stroke where the piston is near TDC, from –25 to +25 ATDC. Although the integrated jet-soot KL does not have any specific physical meaning, it does provide a relative measure of the jet-soot[3] within the path of the LOS beam during the combustion event.

Comparison of the jet-soot levels among the fuels is complicated by differences in the ignition delay, especially at the low-load condition. Fuels that display a longer ignition delay have a somewhat greater time for mixing of fuel and air before combustion. Soot formation is known to be affected by mixture stoichiometry, so differences in jet-soot among the fuels are likely affected by differences in ignition delay as well as changes in soot formation chemistry caused by the fuel additives. Accordingly, a baseline trend of the variation of soot formation with changing ignition delay for the base fuel is needed to properly compare soot formation among the fuel additive blends having different ignition delays.

The ignition delay time can be varied by changing either the fuel chemistry of the base fuel or the thermodynamic conditions of the in-cylinder gases. The first option, changing fuel chemistry to alter the ignition delay (*e.g.,* adding cetane-improving additives), is unattractive because changes in the fuel chemistry could affect soot formation chemistry as well. The second option, changing in the in-cylinder gas thermodynamic state, may also affect the soot formation kinetics, but it was deemed the simplest and least confounding approach. Accordingly, in this study, to provide a baseline of soot formation over a range of ignition delays, the engine was operated with the base fuel (D2), using intake temperatures that yielded ignition delays that spanned the range observed with all of the fuels. To accomplish this, the intake temperature was adjusted to yield TDC temperatures from 800 K to 900 K, which yielded ignition delays with D2 that bounded the ignition delays for all seven fuels at the standard intake conditions, for both low- and high-load conditions. The intake air pressure was also adjusted to maintain a constant TDC charge density as the intake air temperature was changed.

[3] A small amount of wall-soot may also be present, which is deposited during the later part of the cycle, especially for high-load conditions.

The integrated jet-soot KL, plotted versus the ignition delay for each fuel, is shown in Fig. 6. Error bars are included with each data point, which represent the 95% confidence interval for the data. As described above, three different integrated jet-soot KL data points are included for D2, using intake temperatures that yielded ignition delays that spanned the range of all fuels. The dotted lines that connect the D2 data points in Fig. 6 are provided to guide the eye, and they represent the baseline integrated jet-soot KL level for D2, to which the other fuels may be compared. For D2, the integrated jet soot decreases as the ignition-delay increases, especially for the low-load condition. This trend is consistent with the influence of pre-combustion mixing on soot formation, as discussed in the Introduction. As the ignition delay increases, more time is available for mixing, and less soot is formed in the leaner mixtures at ignition. For the low-load condition, a large proportion of the fuel is consumed during the premixed burn, so mixing during the ignition delay is very important for soot formation. For the high-load condition, a greater fraction of the fuel is consumed during mixing-controlled combustion after the premixed burn, so the ignition delay has a much smaller influence on the integrated jet soot.

The fuels display a range of ignition delays and integrated jet-soot levels (especially at low-load). At the low load condition, there are no statistically significant differences in the integrated jet-soot KL between the baseline fuel and the additive mixtures. At the high load condition, only the three fuels containing ethanol (E10, EP10, and EG10) are statistically different than the baseline data after accounting ignition delay effects. That is, although some of the other fuel additives do have an effect on soot formation at the base operating condition, a change in the ignition delay usually accompanies the change in soot formation. As discussed above, the change in ignition delay affects the mixing of fuel and air prior to combustion, which can effect soot formation. For fuel additives other than the three ethanol formulations, the error bars overlap the dependence of soot formation on ignition delay established with D2 (dotted line). Therefore, the non-ethanol fuel additives (G05, NE05, NM05, and S05) affect soot formation primarily through differences in fuel-air mixing prior to combustion, which occurs because of differences in ignition delay. Only the three ethanol-containing additives (E10, EP10, and EG10) display changes to soot formation that cannot be explained by differences in ignition delay alone.

WALL-SOOT DEPOSITION – As discussed earlier, there is significant uncertainty in the jet-soot KL data for dense soot clouds. While the low-load conditions did not display high KL values for any of the fuels tested, the soot cloud became optically thick for all of the high-load conditions, so that significant uncertainty exists in the jet-soot KL data. Furthermore, as discussed earlier, the maximum measurable jet-soot KL was truncated at KL=10. As a result, the integrated jet-soot data for the high-load conditions in Fig. 6 (b) is also likely truncated. As discussed in the Experimental Setup and Diagnostics

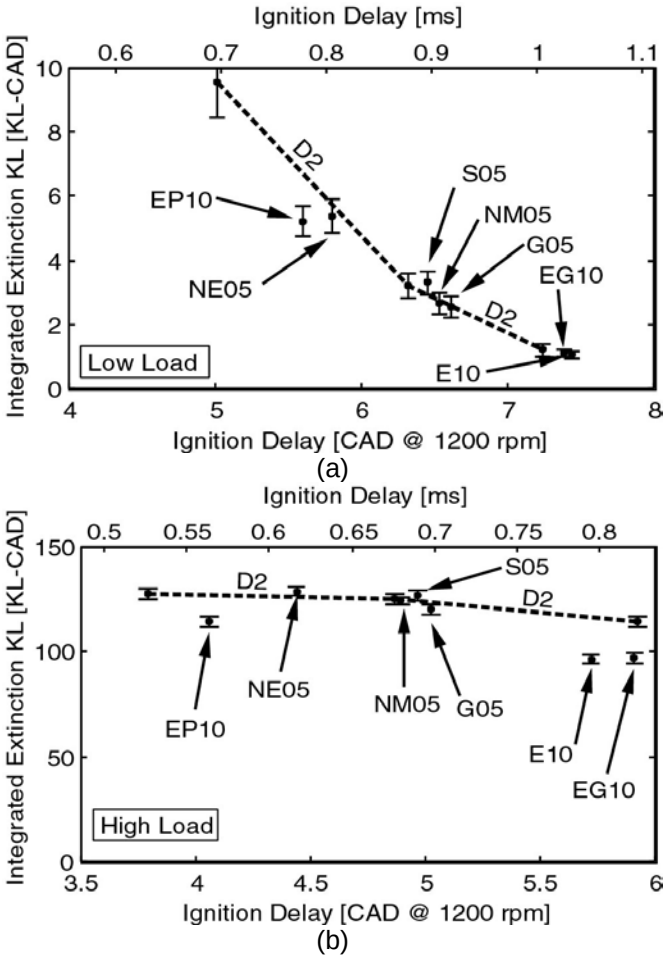

Figure 6. Integrated jet-soot KL for all eight fuels at (a) the low-load and (b) high-load operating conditions. The dotted line is provided to guide the eye for the D2 data, which was acquired at three different conditions, with the intake temperature adjusted to change the ignition delay for D2. The error bars represent the 95% confidence interval for each data point.

section, measurements of wall-soot deposition rates may be used as an alternative criterion to assess diesel soot formation under such highly-sooting conditions.

Shown in Fig. 7 are the wall-soot deposition rate data for all eight fuels at the high-load operating condition. As was done for the integrated jet-soot KL data, the baseline behavior for D2 was established by adjusting the ignition delay using the intake temperature, and the dotted line is provided to guide the eye along the baseline trend for D2. Note that the rate of deposition for this high-load condition is always less than 0.5 KL units per fired cycle. As a result, the KL of the wall-soot does not reach a level with high uncertainty (KL>6) until after at least 12 fired cycles. This illustrates the utility of using the wall-soot deposition rates to acquire data with lower uncertainty than the jet-soot measurements for the highly-sooting, high-load operating conditions.

The trends of the wall-soot deposition data among the eight fuels in Fig. 7 is consistent with the jet-soot data in

Fig. 6; only the ethanol-containing fuels display wall-soot deposition rates that are statistically different than the baseline data. However, since the wall-soot deposition measurements do not suffer from truncation at high KL levels that the jet-soot data did, the differences in wall-soot deposition among the fuels are more apparent. While the integrated jet-soot of the ethanol-containing fuels was 10-15% lower than the baseline, the wall soot-deposition rates for these fuels are 30-40% lower than the baseline.

FLAME LIFT-OFF – As discussed earlier, in addition to the potential chemical kinetic effects that the fuel additives may have on soot formation, they may also affect physical processes that influence soot formation. The significant influence that the diesel flame lift-off length may have on pre-combustion mixing and subsequent soot formation warrants a close examination of differences in the lift-off length among the fuels. As discussed earlier, for the operating conditions of the current study, the flame lift-off length is only meaningful under the high-load operating conditions.

Shown in Fig. 8 are the flame lift-off lengths, which were extracted from OH chemiluminescence images, for all eight of the fuels at the high-load operating condition. The errobars in Fig. 8 represent the uncertainty in the lift-off length measurements, which was established to be about ± 0.5 mm in a previous study [13]. The lift-off lengths range from 7.4 ± 0.5 mm for S05 to 8.3 ± 0.5 mm for EP10. The three ethanol-containing fuels (E10, EP10, and EG10) have among the longest lift-off lengths, and the lowest jet-soot and wall-soot deposition rates (see Figs. 6 and 7). Indeed, for a given fuel, soot formation has been observed to decrease with increasing lift-off length [6]. However, the mean lift-off lengths for these three ethanol-containing fuels are only fractionally larger than that for D2. Such tiny changes in the lift-off length cannot solely be responsible for the 30-40% change in soot formation evident from the soot-wall deposition data (see Fig. 7). For diesel fuels, much larger differences in the lift-off length (>50%) have been observed previously for similar reductions in in-cylinder soot formation [6]. Furthermore, the differences in the mean lift-off lengths are significantly less than the uncertainty in the measurement. Accordingly, there is no statistical difference in the lift-off lengths for these eight fuels at the high-load operating condition that can explain the observed differences in in-cylinder soot.

DISCUSSION

Both the jet-soot data and the wall-soot deposition data indicate that only the ethanol-containing fuels (E10, EP10, and EG10) have a statistically-significant influence on in-cylinder soot formation. The other additive formulations (G05, NE05, and NM05) may indeed affect soot formation chemistry, but they did not have a statistically significant influence on the measured jet-soot or wall-soot for the operating conditions and additive concentrations used in the current study.

Very little difference in the lift-off length was observed among the eight fuels at the high-load operating condition of the current study. This is unexpected, since in single-jet experiments in a constant volume combustion chamber, the thermodynamic state of the ambient gas [2] and fuel characteristics [6] have been shown to have a significant influence on the lift-off length. Furthermore, other fuel additives have been observed to have a significant influence on the lift-off length. For example, in the engine of the present study, the PuriNOx™ water-emulsified diesel fuel from Lubrizol has been observed to have a significantly longer lift-off length than the base fuel from which the emulsion was created [27]. However, the influence of various factors on the lift-off length has been observed to be much

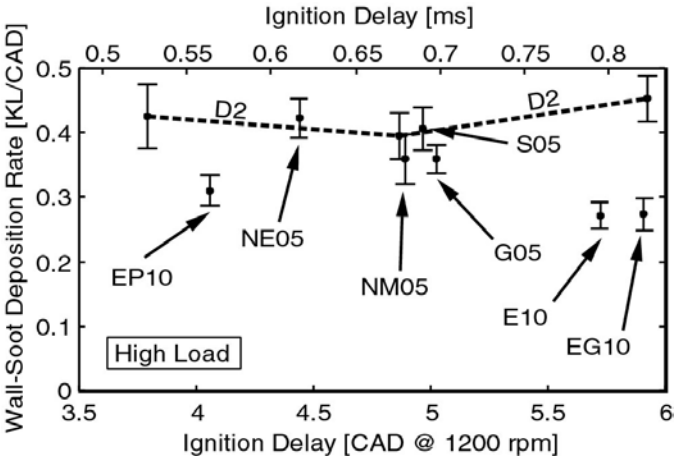

Figure 7. Wall-soot deposition rate for all eight fuels at the high-load operating condition. The dotted line is provided to guide the eye for the D2 data, which was acquired at three different conditions, with the intake temperature adjusted to change the ignition delay for D2. The error bars represent the 95% confidence interval for each data point.

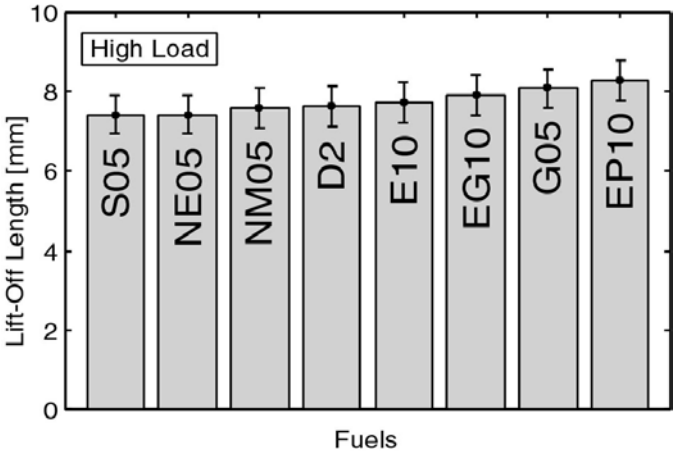

Figure 8. Flame lift-off lengths of all eight fuels at the high-load operating condition. The lift-off length was extracted from images of OH chemiluminescence acquired 2 CAD after the peak in the premixed burn spike. The error bars represent the uncertainty in the lift-off length.

smaller within the in-cylinder environment of this diesel engine under operating conditions similar to those of the current study [8]. The insensitivity of the lift-off length to environmental variables was particularly evident when the lift-off length was short (less than 10 mm). Since all of the measured lift-off lengths were less than 10 mm in the current study, it is possible that fuel-additive effects on the lift-off length may not have been observable at the operating conditions studied. Under other operating conditions that display a generally longer lift-off length, the fuel additives could have an observable influence on the lift-off length, and therefore, on soot formation.

The decreased in-cylinder soot formation observed with increased fuel oxygen content of the ethanol-containing fuels, E10, EP10, and EG10, is consistent with previous observations of exhaust soot in a number of studies of ethanol blends (*e.g.,* see review in Ref. [16]). It is also consistent with previous observations in the facility of the current study, using a range of oxygenated paraffinic fuels. Both the jet-soot and the wall-soot deposition rates were observed to decrease as the oxygen content in the paraffinic fuels was increased [13]. A fuel oxygen content of about 15% by mass yielded a 30-40% decrease in wall-soot deposition rates. If the same correlation were applied to alcohol-diesel blends, then about 40% ethanol by volume would be required to achieve the same reduction in wall-soot. This level is significantly greater than the 10% ethanol content in the additive formulations of the current study, however. Data from the current study is insufficient to explain why the wall-soot deposition rates of ethanol-diesel blends were so much less than for oxygenated paraffinic fuel blends at similar oxygen contents. However, two potential mechanisms are offered that may be responsible for this observation. First, the heat of vaporization of ethanol is over three times that of diesel fuel. As a result, the cooling effect of the vaporizing ethanol may yield significantly colder temperatures in the diesel jet along the path of the LOS laser beam. The reduction in temperature within the jet may inhibit soot formation to some degree [6], and it may also reduce the rate of wall-soot deposition by thermophoresis. Secondly, some chemical kinetic processes may exist for ethanol-diesel blends that either reduce soot formation or inhibit wall deposition. As discussed earlier, molecular structure effects have been shown to be important for soot reduction [6,15,17,28]; the location of oxygen atoms within the fuel molecule can be important. Ethanol may therefore chemically inhibit soot formation more effectively than another fuel with an equivalent oxygen content.

SUMMARY

The influence of several fuel additive formulations on in-cylinder soot formation was investigated in an optically-accessible, heavy-duty DI diesel engine. Fuel additives containing ethanol, ethylene glycol dimethyl ether, polyethylene glycol dinitrate (a cetane improver), as well as nitromethane and another nitro-compound mixture and succinimide (a dispersant) were used at two typical diesel engine operating conditions. In-cylinder soot formation was quantified using a laser-extinction diagnostic, which measured both relative soot concentrations within the jet (“jet-soot”) and soot deposition on in-cylinder surfaces (“wall-soot”). The diesel flame lift-off length was also measured using an OH chemiluminescence imaging diagnostic, to examine differences in pre-combustion mixing among the fuels. Analysis of the data shows:

1. After accounting for differences in ignition delay among the fuels, only the ethanol-containing fuels displayed statistically-significant reduction of soot compared to the base fuel. The ethanol additive reduced jet-soot by up to 15%, and it reduced wall-soot by 30-40%. The ether and nitro-compounds affected ignition delay somewhat, but did not cause any change in soot formation from the base fuel trend.

2. There were no statistically-significant differences in the lift-off lengths among the fuels. Consequently, the observed differences in in-cylinder soot formation among the fuels cannot be attributed to differences in entrainment of fresh oxygen upstream of the flame after the ignition delay period.

3. The surfactant additive had no measurable effect on soot-wall deposition rates.

CONCLUSIONS

At the oxygen contents examined in the current study, only the ethanol-containing fuels displayed a potential for reduction of in-cylinder soot. Either non-ethanol additives have little potential for chemical reduction of in-cylinder soot formation, or their concentrations were too small in the current study to have a significant effect. If economic or other considerations prohibit increasing the blend rates of non-ethanol additives to evaluate their potential at higher concentrations, then their potential for in-cylinder soot reduction is clearly limited.

ACKNOWLEDGMENTS

The authors would like to express their gratitude to David Cicone of Sandia National Laboratories for his assistance with data acquisition and with maintaining and repairing the optical-access research engine used for these experiments.

This work was performed at the Combustion Research Facility, Sandia National Laboratories, Livermore, CA. Support for this work was provided by the Lubrizol Corporation.

REFERENCES

1. Dec, J. E., "A Conceptual Model of D.I. Diesel Combustion Based on Laser-Sheet Imaging," SAE

Paper 970873, SAE Transactions, **106**, No. 3, pp. 1319-1348, 1997.
2. Siebers, D. L. and Higgins, B. S., "Flame Lift-Off on Direct-Injection Diesel Sprays Under Quiescent Conditions," SAE Paper 2001-01-0530, SAE Transactions, **110**, No. 3, pp. 400-421, 2001.
3. Flynn, P. F., Durret, R. P., Hunter, G. L., zur Loye, A. O., Akenyemi, O. C., Dec, J. E., and Westbrook, C. K., "Diesel Combustion: An Integrated View Combining Laser Diagnostics, Chemical Kinetics, and Empirical Validation," SAE Paper 1999-01-0509, SAE Transactions, **108** , 1999.
4. Akihama, K., Takatori, Y., Inagaki, K., Sasaki, S., and Dean, A. M., "Mechanism of the Smokeless Rich Diesel Combustion by Reducing Temperature," SAE Paper 2001-01-0655, SAE Transactions, **110** , No. 3, pp. 648-662, 2001.
5. Pickett, L. M. and Siebers, D. L., "Orifice Diameter Effects on Diesel Fuel Jet Flame Structure," Proceedings of the Fall Technical Conference of the ASME Internal Combustion Engine Division, 2001.
6. Pickett, L. M. and Siebers, D. L., "Fuel Effects on Soot Processes on Fuel Jets at DI Diesel Conditions," SAE Paper 2003-01-3080, 2003.
7. Higgins, B. and Siebers, D., "Measurement of the Flame Lift-Off Location on D.I. Diesel Sprays using OH Chemiluminescence," SAE Paper 2001-01-0918, SAE Transactions, **110**, No. 3, pp. 739-753, 2001.
8. Musculus, M. P. B., "Effects of the In-Cylinder Environment on Diffusion Flame Lift-Off in a DI Diesel Engine," SAE Paper 2003-01-0074, 2003.
9. Zhao, H. and Ladommatos, N., "Optical Diagnostics for Soot and Temperature Measurement in Diesel Engines," Prog.Energy Combust.Sci., **24**, pp. 221-255, 1998.
10. Dec, J. E., Canaan, R. E., and Tree, D. R., "The Effect of Water-Emulsified Fuel on Diesel Soot Formation," 219th ACS National Meeting, San Francisco, CA, 2000.
11. Tree, D. R. and Dec, J. E., "Line-of-Sight Extinction Measurements of Oxygenated Fuel Blends and Diesel Fuel in a Heavy-Duty, Direct-Injection Diesel Engine," 2nd Joint Meeting of the United States Sections of The Combustion Institute, Oakland, CA, 2001.
12. Tree, D. R. and Dec, J. E., "Extinction Measurements of In-Cylinder Soot Deposition in a Heavy-Duty DI Diesel Engine," SAE Paper 2001-01-1296, SAE Transactions, **110**, 2001.
13. Musculus, M. P. B., Dec, J. E., and Tree, D. R., "Effects of Fuel Parameters and Diffusion Flame Lift-Off on Soot Formation in a Heavy-Duty Diesel Engine," SAE Paper 2002-01-0889, SAE Transactions, **111**, 2002.
14. Dec, J. E. and Tree, D. R., "Diffusion-Flame / Wall Interactions in a Heavy-Duty DI Diesel Engine," SAE Paper 2001-01-1295, 2001.
15. Natarajan, M., Frame, E. A., Naegeli, D. W., Asmus, T., Clark, W., Garbak, J., Gonzalez, M. A., Liney, E., Piel, W., and Wallace III, J. A., "Oxygenates for Advance Petroleum-Base Diesel Fuels: Part 1. Screening and Selection Methodology for the Oxygenates," SAE Paper 2001-01-3631, SAE Transactions, **110**, No. 4, 2001.
16. Corkwell, K. C., Jackson, M. M, and Daly, D. T., "Review of Exhaust Emissions of Compression Ignition Engines Operating on E Diesel Fuel Blends," SAE Paper 2003-01-3283, 2003.
17. Mueller, C. J. and Martin, G. C., "Effects of Oxygenated Compounds on Combustion and Soot Evolution in a DI Diesel Engine: Broadband Natural Luminosity Imaging," SAE Paper 2002-01-1631, SAE Transactions, **111**, No. 4, 2002.
18. Bush, K. C., Germane, G. J., and Hess, G. L., "Improved Utilization of Nitromethane as an Internal Combustion Engine Fuel," SAE Paper 852130, 1985.
19. zur Loye, A. O., Siebers, D. L., McKinley, T. L., Ng, H. K., and Primus, R. J., "Cycle-Resolved LDV Measurements in a Motored Diesel Engine and Comparisons with k-epsilon Model Predictions," SAE Paper 890618, SAE Transactions, **96**, No. 3, pp. 1142-1158, 1989.
20. Espey, C. and Dec, J. E., "Diesel Engine Combustion Studies in a Newly Designed Optical-Access Engine Using High-Speed Visualization and 2-D Laser Imaging," SAE Paper 930971, SAE Transactions, **99**, No. 4, pp. 703-723, 1993.
21. Musculus, M. P. B. and Pickett, L. M., "Diagnostic Considerations for Optical Laser-Extinction Measurements of Soot in High-Pressure Combustion Environments," Submitted to Combustion and Flame, 2004.
22. Jenkins, F. A. and White, H. E., *Fundamentals of Optics*, McGraw-Hill, Inc., 1981.
23. Dec, J. E. and Espey, C., "Chemiluminescence Imaging of Autoignition in a D.I. Diesel Engine," SAE Paper 982685, 1998.
24. Heywood, J. B., *Internal Combustion Engine Fundamentals*, McGraw-Hill, Inc., 1988.
25. Espey, C. and Dec, J. E., "The Effect of TDC Temperature and Density on the Liquid-Phase Fuel Penetration in a D.I. Diesel Engine," SAE Paper 952456, SAE Transactions, **104**, No. 4, 1995.
26. Bethea, R. M., Duran, B. S., and Boullion, T. L., *Statistical Methods for Engineers and Scientists*, 2 Edition, Owen, B. Editors, Marcel Dekker, Inc., New York, New York, 1985.
27. Musculus, M. P. B., Dec, J. E., Tree, D. R., Daly, D., Langer, D., Ryan, T. W. III, and Matheaus, A. C., "Effects of Water-Fuel Emulsions on Spray and Combustion Processes in a Heavy-Duty DI Diesel Engine," SAE Paper 2002-01-2892, SAE Transactions, **111**, pp. 2736-2756, 2002.
28. Buchholz, B. A., Mueller, C. J., Upatnieks, A. Martin G. C., Pitz, W. J., and Westbrook, C. K., "Using Carbon-14 Isotope Tracing to Investigate Molecular Structure Effects of the Oxygenate Dibutyl Maleate on Soot Emissions from a DI Diesel Engine," SAE Paper 2004-01-1849, 2004.

ACRONYMS

AHRR	Apparent Heat Release Rate
ATDC	After Top Dead Center
BPF	Band Pass Filter
CAD	Crank Angle Degrees
CW	Continuous Wave
D2	Diesel fuel no. 2 (generic)
E10	Fuel blend of D2 with 10% Ethanol by weight
EG10	D2 + 10% Ethanol + 0.5 % EGDE
EGDE	Ethylene Glycol Dimethyl Ether
EP10	D2 + 7.5% Ethanol + 2.5% PEGDN
FWHM	Full Width at Half Maximum
G05	D2 + 0.5% EGDE
GIMEP	Gross Indicated Mean Effective Pressure
ICCD	Intensified Charge Coupled Device
KL	natural log optical density (Eq. 1)
LOS	Line-Of-Sight
NE05	D2 + 0.5% 2002-20605 nitro compound
NM05	D2 + 0.5% nitromethane
PEGDN	Polyethylene Glycol Dinitrate
PM	Particulate Matter
S05	D2 + 0.5% Succinimide dispersant
TDC	Top Dead Center
UV	UltraViolet

APPENDIX: SUPPLEMENTARY FIGURES

Each figure in the appendix shows the transmissivity (solid line), jet-soot KL (solid line with error bars) and AHRR (dotted line, for reference) for each fuel and operating condition, as indicated in the upper right corner of each plot. The error bars represent the 95% confidence interval for the 192 cycles of data acquired, based on cycle-to-cycle variability only.

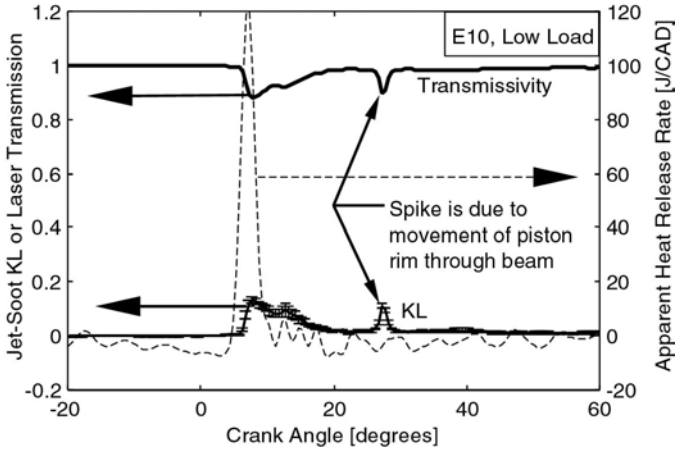

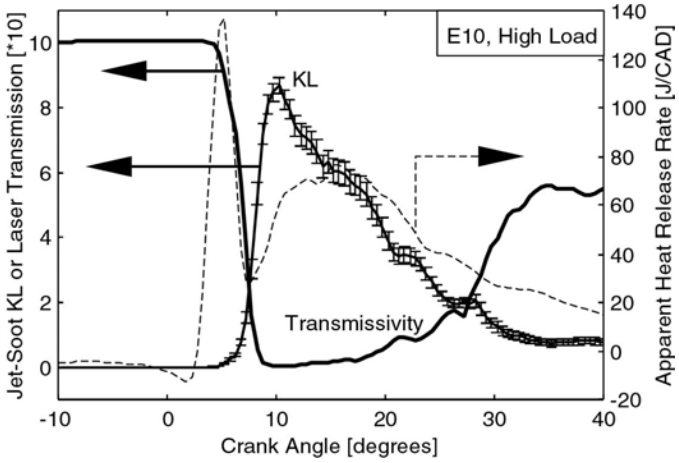

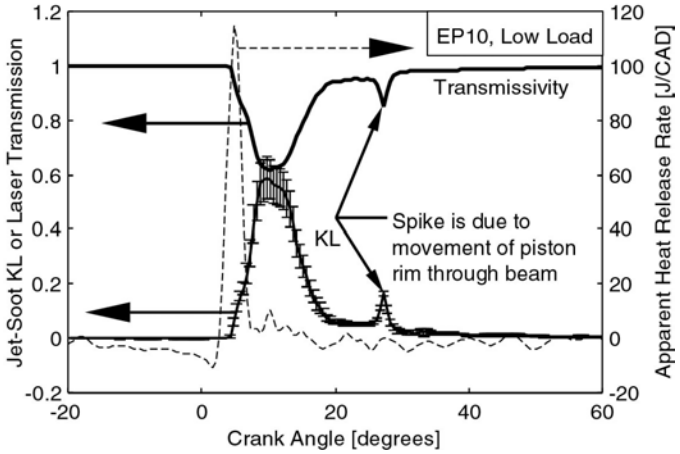

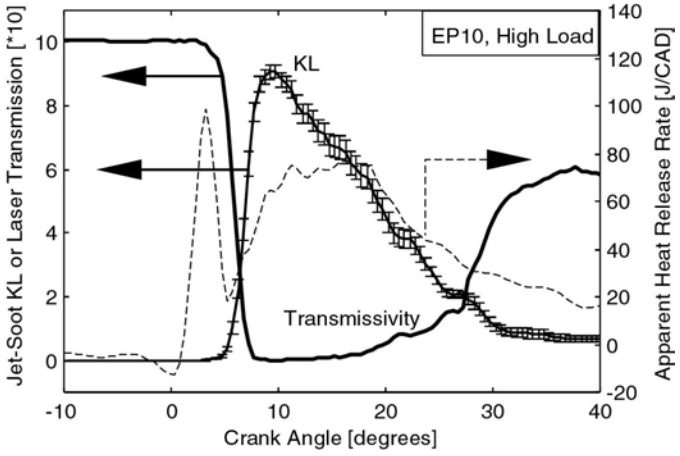

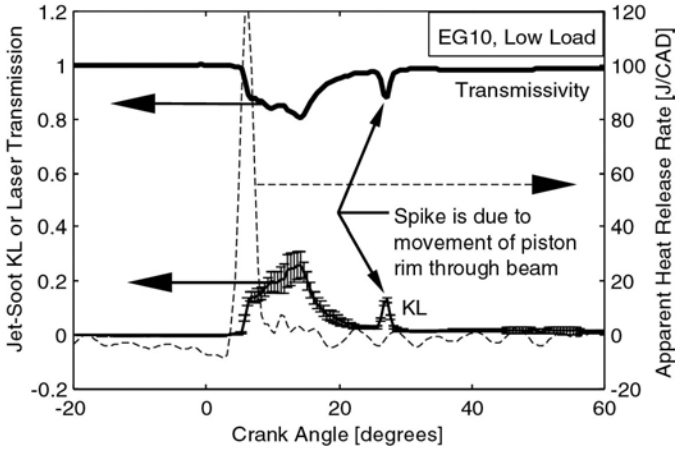

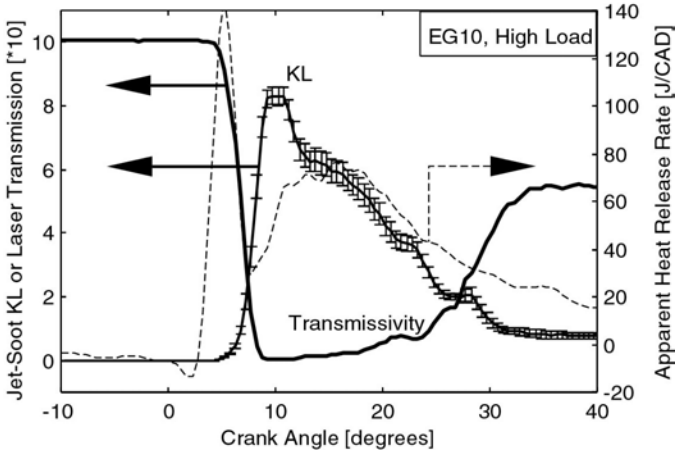

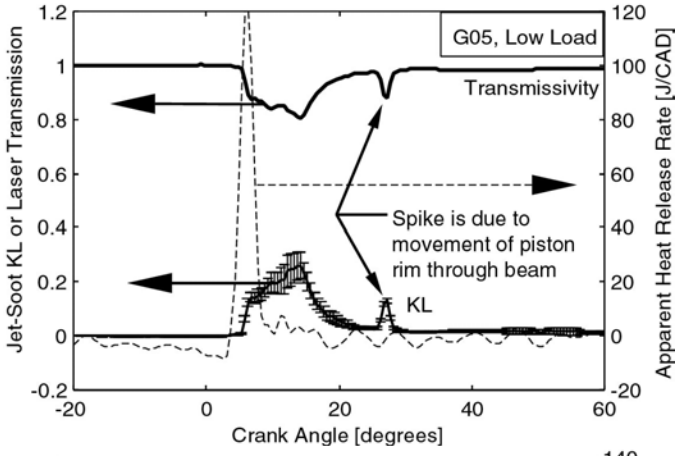
G05, Low Load
Transmissivity
Spike is due to
movement of piston
rim through beam
KL
Jet-Soot KL or Laser Transmission
Apparent Heat Release Rate [J/CAD]
Crank Angle [degrees]

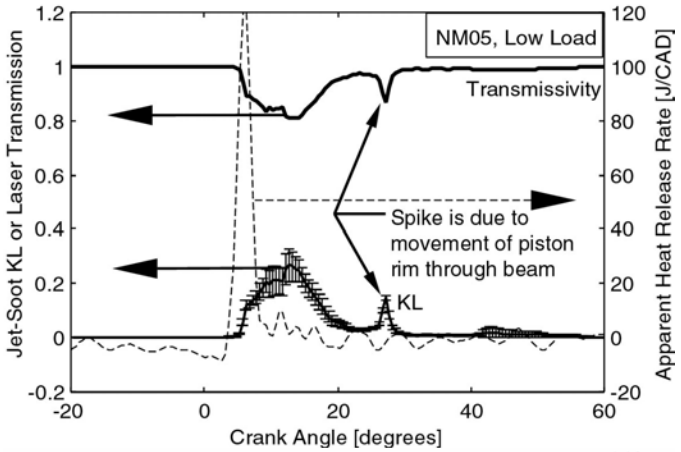
NM05, Low Load
Transmissivity
Spike is due to
movement of piston
rim through beam
KL
Jet-Soot KL or Laser Transmission
Apparent Heat Release Rate [J/CAD]
Crank Angle [degrees]

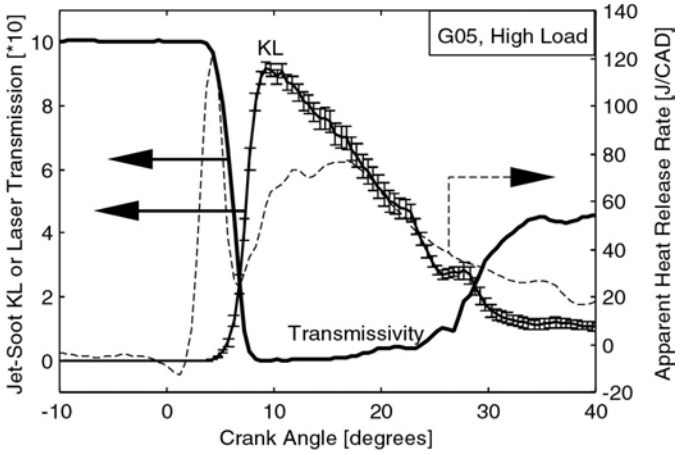
G05, High Load
KL
Transmissivity
Jet-Soot KL or Laser Transmission [*10]
Apparent Heat Release Rate [J/CAD]
Crank Angle [degrees]

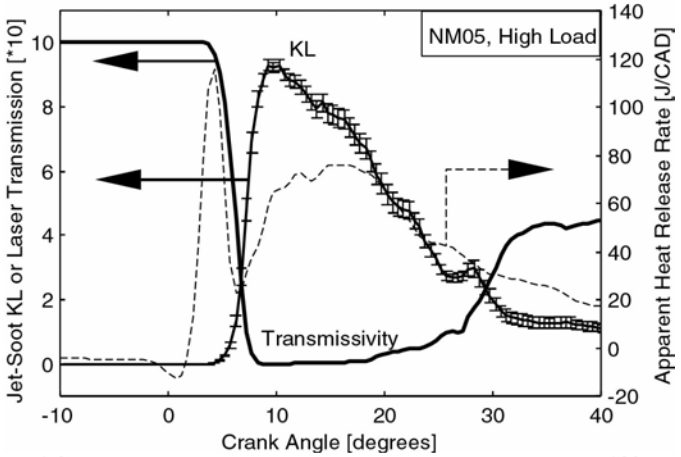
NM05, High Load
KL
Transmissivity
Jet-Soot KL or Laser Transmission [*10]
Apparent Heat Release Rate [J/CAD]
Crank Angle [degrees]

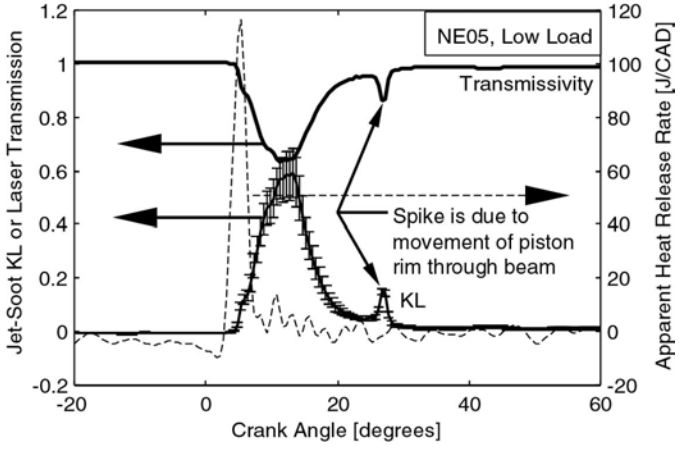
NE05, Low Load
Transmissivity
Spike is due to
movement of piston
rim through beam
KL
Jet-Soot KL or Laser Transmission
Apparent Heat Release Rate [J/CAD]
Crank Angle [degrees]

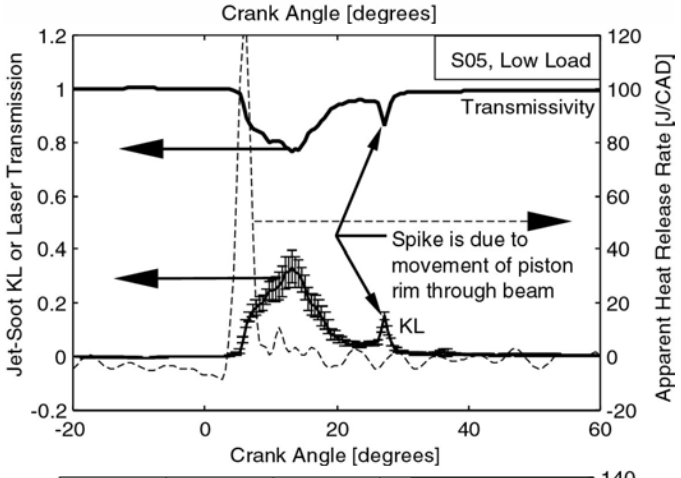
S05, Low Load
Transmissivity
Spike is due to
movement of piston
rim through beam
KL
Jet-Soot KL or Laser Transmission
Apparent Heat Release Rate [J/CAD]
Crank Angle [degrees]

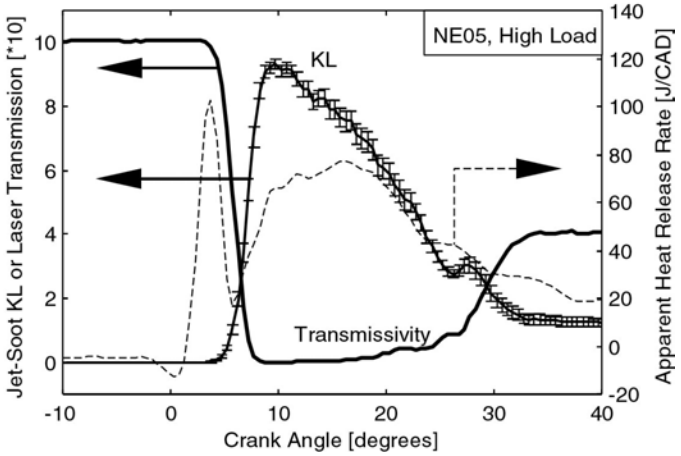
NE05, High Load
KL
Transmissivity
Jet-Soot KL or Laser Transmission [*10]
Apparent Heat Release Rate [J/CAD]
Crank Angle [degrees]

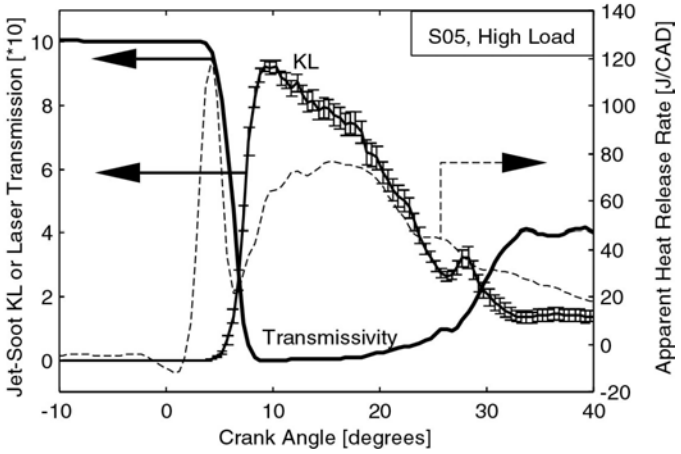
S05, High Load
KL
Transmissivity
Jet-Soot KL or Laser Transmission [*10]
Apparent Heat Release Rate [J/CAD]
Crank Angle [degrees]